Regimes of Liquid Rope Coiling Instability

Classifying the coiling dynamics effect of a viscous fluid

Daniela Molina
Flow Visualization
Professor Jean Hertzberg
Spring 2011

I. Introduction

This image typifies the beginning of the instability called "liquid rope coiling" by Barnes and Woodcock [1], whose groundbreaking work was the first experimental investigation in a series spanning almost 50 years. The image was captured for the Flow Visualization course first project, "Get Wet", at the University of Colorado at Boulder with the intent to make the physics of the flowing liquid visible. The study of this phenomenon is, in nature, very complex despite its simple and innate flow. This report will explain and describe in detail the physics and forces that govern the "liquid rope coiling" instability and will determine what regime this specific case embodies in order to understand the properties of such viscous liquid rendered in this image.

II. Technique

In this setup, silicon oil, a highly viscous liquid with density ρ, and viscosity ν, flows at a volumetric rate Q, through a central hole with diameter d in a partition inside a rectangular vessel filled with air. The dynamics phenomena of liquid rope coiling can be closely observed as the liquid makes its way through the hole and slowly falls a distance H to the flat surface of the vessel and continually falls on its own viscous surface as it transitions to fill the air partition. Figure 2 shows a close up of the detailed measurements of the liquid dynamics that will be analyzed.

The experimental arrangement to capture the image is illustrated in Figure 1. The rectangular vessel is composed of 6 compartments, completely isolated horizontally and joined vertically through a central hole. Each pair of joined compartments is filled with a different color dyed silicon oil (yellow, blue and red) and air. Each compartment acts in the same manner, but the image is focused on the blue dyed silicon oil compartments. The vessel was placed against a black background in a relatively low light area and was top lit with a 17-LED flashlight of 68 lumens. The flashlight was positioned directly on the red dyed silicon oil compartments to create the colored light reflections seen in the image.

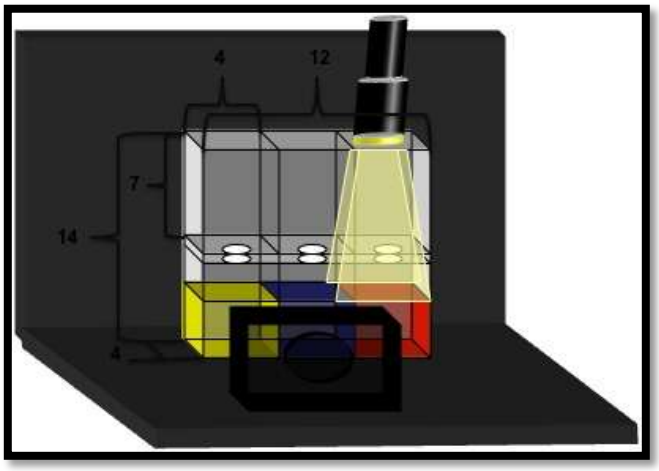

Figure 1: The camera's lens was kept to its minimum focal length (6mm) and was located directly on the surface of the rectangular vessel. Likewise, the 17-LED flashlight was directly placed on top of the red silicon oil compartment.
*Note: All dimensions are in units of centimeters

The camera used for the collection of the image was a digital PowerShot SX120 IS Canon. The camera's lens was place directly on the clear wall surface of the rectangular vessel to avoid any optical zooming and loss of qualitative information due to image granulation from the magnification. Thus, the focal length was left at its minimum of 6mm. The original image had pixel dimensions of [X: 1600, Y: 1200] and a resolution of pixel/inch of [X: 72, Y: 72]. When capturing the image, the camera was set to manual operation to adjust the exposure settings accordingly to the access of light, movement of the liquid and best focus to record the wanted details. The shutter speed was 1/15sec, the aperture value was f/3.5 and the ISO speed rating was 800 (half of the camera's maximum) to decrease the image noise and run a slower film, however still maintaining a relatively good sensitivity to light to balance the other lower exposure settings and low light environment. The maximum aperture value was f/2.7 and the

camera's flash did not fire. The image was edited in Photoshop; it was cropped, and the saturation and contrast were adjusted to highlight and focus on the physical flow and details of interest to demonstrate the instability dynamics at study. The resulting edited image had pixel dimensions of [X: 1173, Y: 1357], and the resolution was kept the same as the original image.

III. Analysis

When the rectangular vessel is flipped and the silicon oil begins to fall after the air has transitioned through the partition hole, the stream of liquid falls straight until it hits the bottom surface of the vessel. Once the liquid comes in contact with the surface, it starts to form a helical coil and the angular coiling frequency Ω, stars to act. The liquid forms a liquid rope coil that comprises of a long nearly vertical "tail" and a helical "coil" of radius R on the surface described in Figure 2[2]. The first theoretical advance towards the understanding of liquid rope coiling was Taylor's [3] recognition that the instability is fundamentally a buckling instability like that of an elastic rod under an applied compressive stress. Succeeding theoretical studies based on linear stability analysis determined the critical fall height and frequency at the onset of coiling [4][5]. In more recent years, Mahadevan et al. [6] was the first to successfully explain finite-amplitude coiling by showing that rapid coiling is governed by a scaling law involving a balance between rotational inertia and the viscous forces resisting the bending of the rope. Ribe [7], however, in his most recent studies of this phenomenon, showed that this scaling is only one of several that are feasible for liquid ropes. Ribe showed that coiling can occur in three distinct regimes: viscous, gravitational and inertial, depending on the relative magnitudes of these respective forces (F_V, F_G, F_I) acting on the rope and a multi-valued coiling frequency at a fixed height. The multi-valued frequency was investigated in more detail by Ribe et al. [8] finding that this multi-valued coiling corresponded to a distinct inertio-gravitational regime in which the rope behaves as a distributed pendulum. The dynamical regime in which coiling takes place per unit length of the rope are determined by the following [7]:

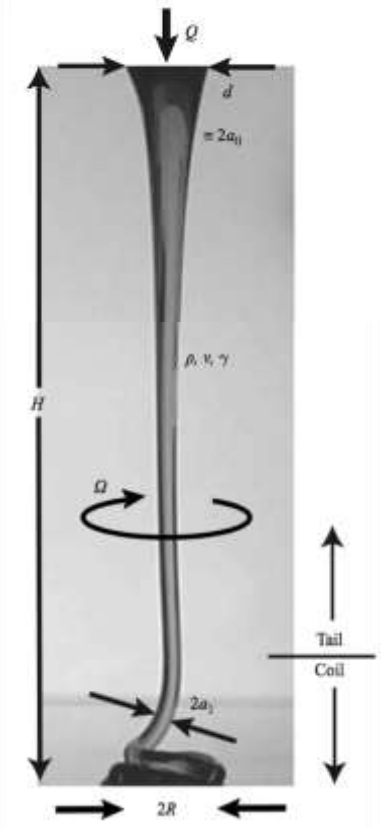

Figure 2

$$F_V \sim \rho \nu a_1^4 U_1 R^{-4}, \quad F_G \sim \rho g a_1^2, \quad F_I \sim \rho a_1^2 U_1^2 R^{-1}$$

where $a_1$is the radius of the rope within the coil and $U_1 = Q/\pi a_1^2$ is the corresponding axial velocity of the fluid. Due to the fact that the radius of the rope is close to constant in the coil, a_1 is defined to be at the point of contact with the vessel surface as depicted in Figure 2.

In this setup, $\rho = 0.97$ g cm^{-3} for silicon oil. The kinematic viscosity ν of an estimated magnitude of 1000 cm^2 s^{-1} fell at a mean volumetric rate Q = 0.013 cm^3 s^{-1} through a hole of diameter d=1.27cm (in the center of the partition) from a distance H = 7cm. The radius of the liquid rope at its point of contact with the vessel a_1 = 0.3 cm. With a fixed distance of fall H, the range of height, $H(g/\nu^2)^{1/3}$ = 0.70, was determined to classify the coiling regime this instability in the rectangular vessel epitomizes. For 0.4 m ≤ $H(g/\nu^2)^{1/3}$ ≤ 1.2 m, viscous forces in the coil are balanced by both gravity and inertia, giving rise to a complex transitional regime: inertio-gravitational regime [2]. The dynamic of the falling liquid is determined by the balance of the forces acting on the tail portion of the rope, which behaves like a spiraling viscous string that deforms primarily by stretching. Viscosity, gravity, and centrifugal inertia that resist stretching are all important forces acting on the falling liquid. At a fixed height, coiling usually occurs with different frequencies, each of which is proportional to the familiar pendulum frequency [2]:

$$\Omega_{IG} = \left(\frac{g}{H}\right)^{1/2}$$

Thus, with a fixed height of 7 cm in the rectangular vessel, the silicon oil liquid coil rope experiences an inertio-gravitational frequency Ω_{IG} = 11.83 Hz. Further, with a coil base of radius R=1.5 cm, the viscous, gravitational and inertial forces individual magnitudes acting on the liquid flow are defined as $F_V \sim 7.14\text{x}10^{-5}$ N, $F_G \sim 0.0856$ N, $F_I \sim 1.23\text{x}10^{-7}$N.

IV. Conclusions

The phenomenon of "liquid rope coiling" instability has been discussed in detail and applied to the fluid at study. After analyzing the measurements taken of the fluid dynamics and determining the height range of the liquid, conclusions where made by classifying the behavior of what the image captured as an inertio-gravitational coil regime. Before even plunging into specific phenomenon effects of the flow, the Reynolds number of the liquid, being of a small value (R_e<2300) indicated a laminar flow, which states a dominance of the viscous forces. In this case, after further research of coiling instability, these viscous forces are also being balanced by gravitational and inertial forces acting on the tail portion of the flow deforming primarily by stretching, unlike the other three regimes which act on the coil portion and deform primarily by twisting and bending.

In closing, it is incredible to think that behind such a simple concept of a falling viscous liquid, there is such a complex world of dynamics and physics. This is a snapshot in time of a falling liquid that would, in most probable cases, be taken for granted or would not be acknowledged for its beauty and complexity. However, this image, in its simplest form, causes the mind to further question what it is capturing; and in its elaborated form, it uncovers a phenomenon of one of the most intricate regimes of the liquid rope coil instability.

[1] G. Barnes and R. Woodcock, Am. J. Phys. 26, 205 (1958).
[2] N.M. Ribe, H.E. Huppert, M.A. Hallworth, M. Habibi and D.Bonn, J. Fluid Mech., 555 (2006).
[3] G.I. Taylor, Proceedings of the 12th International Congress of Applied Mechanics (Berlin, Springer, 1968).
[4] J.O. Cruickshank, J. Fluid Mech. 193, 111 (1988).
[5] B. Tchavdarov, A.L. Yarin, and S. Radev, J. Fluid Mech. 253, 593 (1993).
[6] L. Mahadevan, W.S. Ryu, and A.D.T. Samuel, Nature (London) 392, 140 (1998).
[7] N.M. Ribe, Proc. R. Soc. London, Ser. A 460, 3223 (2004).
[8] N. M. Ribe et al., J. Fluid Mech. 555, 275 (2006).